

SPATIAL DIFFUSION OF WEAKLY BOTTLENECKED 29 cm^{-1} PHONONS
IN RUBY OBSERVED BY QUASI-STATIONARY TECHNIQUES

J.I. Dijkhuis and H.W. de Wijn

Fysisch Laboratorium, Rijksuniversiteit, P.O.Box 80.000, 3508 TA Utrecht, The Netherlands

(Received 11 April 1979 by A.R. Miedema)

In weakly bottlenecked ruby the decay of 29 cm^{-1} phonons is found to occur through spatial diffusion to the edge of the excitation zone, also when the phonon packets are fully separated in a magnetic field. The regime of very weak bottlenecking could be disclosed for experiment by a new technique, based on quasi-stationary tracking of the R_1 and R_2 fluorescence after switching on strong optical pumping.

DUE TO the very short lifetime of the $2\bar{A}(^2E)$ level in ruby against decay to $\bar{E}(^2E)$ under emission of a phonon ($T_{2\bar{A}\rightarrow\bar{E}} \approx 1\text{ ns}$), as compared to the radiative decay time ($\tau_R \approx 4\text{ ms}$), the fluorescence emanating from $2\bar{A}$ at pumped liquid helium temperatures usually disappears into the background. In stationary experiments,^{1,2} the R_2 fluorescence could only be observed in case of a strong bottleneck of the 29 cm^{-1} phonons, when the decay of $2\bar{A}$ is considerably slowed down, *i.e.*, the spontaneous $T_{2\bar{A}\rightarrow\bar{E}}$ is prolonged to $T_{2\bar{A}\rightarrow\bar{E}}^{\text{eff}}$ by the bottlenecking factor σ . The region of low bottlenecking, which is a primary point of interest in this letter, has remained inaccessible to continuous measurements. We have developed a new quasi-stationary measuring technique exploiting the ability of the $2\bar{A}$ population, $N_{2\bar{A}}$, to rapidly reach equilibrium with \bar{E} . The key of the method is to stepwise apply *full* optical pumping, and to observe, while the metastable population N^* increases, the development of both the R_1 and R_2 intensities on a time scale large compared to $T_{2\bar{A}\rightarrow\bar{E}}$. Thus, already at low σ , just following the switching on of the pumping, the feeding rate ϕ into $2\bar{A}$, and thereby the generation of 29 cm^{-1} phonons, is maximum. Since

$$N_{2\bar{A}} = \phi T_{2\bar{A}\rightarrow\bar{E}}^{\text{eff}}, \quad (1)$$

as may be seen from balancing feeding and decay of $2\bar{A}$, the R_2 intensity is amplified by a factor equal to ϕ over the feeding rate into $2\bar{A}$ that in a stationary experiment would establish the same $N_{\bar{E}}$. In practice this factor may amount to ~ 1000 . After a time somewhat larger than τ_R , saturation will, of course, be reached at a ratio $N_{2\bar{A}}/N_{\bar{E}}$ essentially equal to stationary pumping at full power. Switching off the pumping, R_1 decays with τ_R , while R_2 almost instantaneously disappears with $T_{2\bar{A}\rightarrow\bar{E}}^{\text{eff}}$.³ After the excited states have been depleted, a new cycle may be started, allowing to take advantage of repetitive signal averaging techniques.

In the actual experimental set-up, the pump argon-laser beam, incident perpendicular to the c axis, is chopped by use of an acousto-optical crystal. In first-order deflection, rectangular

light pulses of tunable duration are obtained with a risetime of $\sim 0.2\ \mu\text{s}$ and a suppression ratio of 3000, which essentially is an upper limit of the factor that can be gained in detecting R_2 . The R_1 and R_2 fluorescent lines are observed at right angles to the laser beam and the c axis. They are selected by a double monochromator, preferentially sensitive to polarizations transverse to the c axis, and followed by standard photon-counting apparatus. The detection chain is terminated by a multi-channel analyzer, recording the time evolution of the fluorescence selected. The time, taken as parameter, is finally eliminated to arrive at the dependence of the R_2 fluorescent intensity on that of R_1 . A typical result for the dependence of R_2 on R_1 in a 700 ppm crystal at 1.5 K, averaged over 50000 sweeps, is presented in Fig.1. The pulse length applied was 12 ms, while the duration of the light-off period was set at 60 ms to allow the metastable population to decay sufficiently. To avoid overload when detecting the strong R_1 fluorescence, neutral density filters were used, and subsequently accounted for in the R_1 scale. The background, determined by recording the fluorescence emitted beside the R_1 and R_2 lines, is subtracted. To determine σ , which is proportional to R_2 according to Eq.(1) and

$$\sigma = T_{2\bar{A}\rightarrow\bar{E}}^{\text{eff}}/T_{2\bar{A}\rightarrow\bar{E}}, \quad (2)$$

we resort to R_2/R_1 reached in the limit of saturation. Then, $\phi = 0.28 N_{\bar{E}} \tau_R$, where the factor 0.28 in the numerator represents the fraction of the optical feeding into $2\bar{A}$,⁴ $N_{\bar{E}} \approx N^*$, and $\tau_R \approx 6.4\text{ ms}$, enhanced from 4 ms by reabsorption. Converting the peak intensities in Fig.1 to integrated ones (Note that the integrated R_2/R_1 is about half the peak R_2/R_1 in the configuration used), and taking into account the various matrix elements of the transition,⁵ we arrive at the σ scale at the right-hand side of Fig.1.

We first discuss Fig.1 in relation to earlier experiments in the continuous mode.¹ In the high-bottlenecking regime a 1.2-power dependence

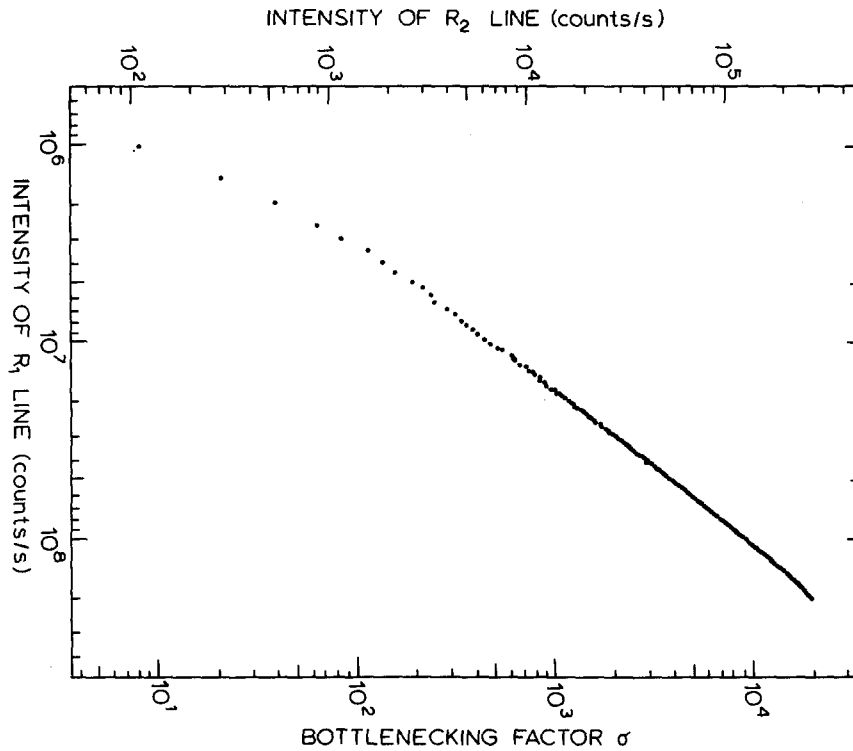


Fig.1. The peak intensity of the R_2 line vs. that of R_1 in a quasi-stationary experiment at 1.5 K, obtained after 50000 passes. The σ scale is anchored to R_2 at high pumping levels. Data points are obtained at 12.5 μs intervals; logarithmic plotting and approach of saturation result in merging of points at high intensities.

is found over at least 2 decades of σ , while at low σ a second power is observed. The latter part corresponds to diffusion limited phonon transport to the boundary, and will be considered further below. At higher σ , the present findings are indeed comparable with the earlier continuous experiments, in which the dependence of R_2 on R_1 was found to have an exponent 2.1 ± 0.1 . Notice that in the experiments with continuous pumping, σ is proportional to the ratio R_2/R_1 , whereas with the present technique, where ϕ is a constant rather than proportional to N^* , σ scales with R_2 itself, making a difference of unity in the exponent.

(i) R_2 vs. R_1 at low bottlenecking. Having established the consistency of the quasi-stationary technique with continuous experiments at higher σ , we subsequently discuss the low-bottlenecking regime. The data at low σ are represented to better advantage in Fig.2, where σ is plotted linearly vs. N^* . The full drawn curve is a fit to the data assuming pure spatially diffusive phonon transport to the edge of the cylindrical excitation region. Working out the corresponding diffusion equation for N_{2A}^2 ,² spatially averaging over the cylinder of excitation, and applying Eq.(1), we find

$$\frac{T_{2A \rightarrow E}^{\text{eff}}}{T_{2A \rightarrow E}} = (3/8)\xi^2 + 1, \quad (3)$$

where the unit term is a correction due to Milne,⁶ expressing that $T_{2A \rightarrow E}^{\text{eff}}$ can never become shorter than $T_{2A \rightarrow E}$; the dimensionless quantity $\xi = R/\lambda$,

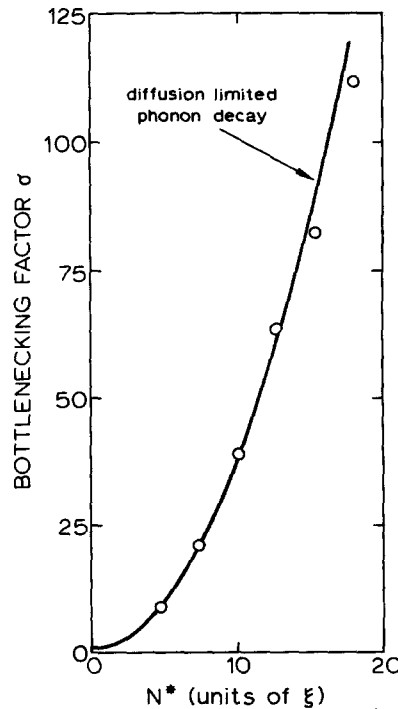


Fig.2. The bottlenecking factor σ vs. N^* in the regime of diffusive phonon transport. The horizontal scale is in units of the opacity ξ for resonant phonons, according to a fit of Eqs.(2) and (3) to the data.

with R the radius of the cylinder and Λ the mean free path, is the "opacity" of the excited region for transport of energy by resonant phonons; Λ , in turn, is related to N^* through $\Lambda = v\rho\Delta v T_{2\bar{A} \rightarrow \bar{E}} / N^*$, with v the speed of sound and $\rho\Delta v$ the number of phonon modes on speaking terms (For simplicity, we do not distinguish between various polarizations and directions of travel).

In Fig.2, the full curve represents Eq.(3) after adjustment to the data points in the low bottlenecking regime, with Eq.(2) used to convert $T_{2\bar{A} \rightarrow \bar{E}}^{\text{eff}}$ to σ . The fit confirms the idea that at low bottlenecking and in a restricted excitation zone, phonon decay is predominantly by spatial diffusion. Indications for such a decay, under roughly the same conditions, were earlier found with time-resolved experiments³ in the form of a raised $T_{2\bar{A} \rightarrow \bar{E}}^{\text{eff}}$ at higher pump power. More concrete evidence for spatial diffusion, yet at higher σ , was obtained in stationary experiments² with an excitation region of diameter $\sim 0.1 \text{ mm}$. At this point, it is of interest to compare the diffusion constant for transport of 29 cm^{-1} excitation,²

$$D_{2\bar{A}} = (v\rho\Delta v)^2 T_{2\bar{A} \rightarrow \bar{E}} / 3N^{*2} \quad (4)$$

derived from the present low-bottleneck experiments with the one obtained from the stationary experiments at higher pumping. This requires tying together the N^* 's in the two experiments, which can reasonably be done by comparing the saturation characteristics of R_1 on laser power. The maximum N^* attained in Fig.2 then is $\sim 0.5\%$ of the maximum N^* for 700 ppm ruby in Ref.2. Taking into account the difference in R in the two experiments, we see that in the present experiments $D_{2\bar{A}} N^{*2}$ is at least 5 times smaller than in the stationary experiments at higher σ , *i.e.*, at low bottlenecking the probability per Cr^{3+} in the \bar{E} state for interruption of 29 cm^{-1} excitation is larger. In view of Eq.(4), this apparently indicates that $\rho\Delta v$, *i.e.*, the number of phonon modes active in transporting the energy released in the non-radiative decay $2\bar{A} \rightarrow \bar{E}$ to the edge of the zone, increases with bottlenecking. There is more direct evidence for this in the heat-pulse experiments of Kaplyanskii *et al.*⁷ They let ballistic phonon pulses propagate through excited ruby in various crystallographic directions, which revealed a strong anisotropy of the coupling between phonons and Cr^{3+} in the \bar{E} state. Thus, due to weaker coupling, at relatively low bottle-

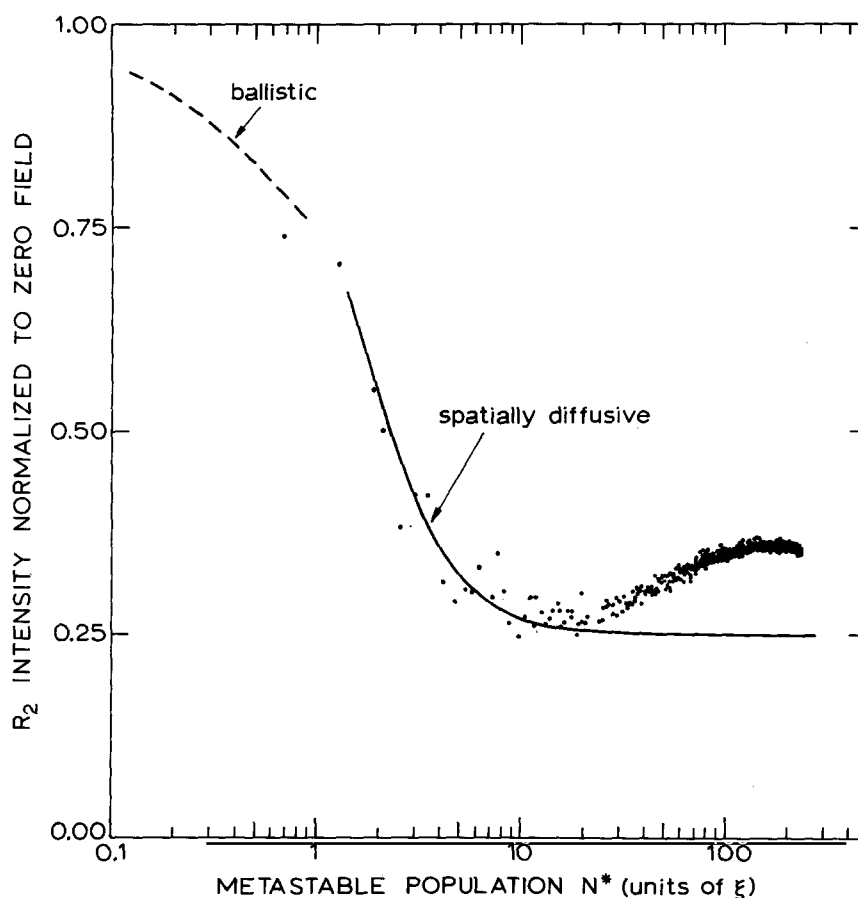


Fig.3. The intensity of the R_2 line at 2 kG normalized to zero field vs. N^* . The full curve is a fit of Eq.(5) to the data, calibrating the horizontal scale in units of the opacity ξ ; the dashed curve is Eq.(6).

necking a good fraction of the phonon modes are not yet involved in carrying off energy.

(ii) R_2 vs. R_1 in a magnetic field. On applying a magnetic field of, say, 2 kG along the c axis, the $2\bar{A} \leftrightarrow \bar{E}$ line splits in four well-separated transitions, each of which is on speaking terms with its own phonon packet. Under these circumstances, the number of Cr^{3+} ions able to absorb a particular phonon is reduced by a factor of two. The corresponding drop of σ has been reported on earlier¹ in the regime of high bottlenecking, as it was tracked through the reduction of R_2 fluorescence with field under continuous pumping. Here, we will consider a typical result for the R_2 intensity at 2 kG normalized to zero field in the region of low bottlenecking, as obtained with the present quasi-stationary technique. Figure 3 has been made up from the results of three consecutive runs, in which the time evolutions of the R_1 line, the R_2 line at zero field, and the R_2 line at 2 kG were recorded, otherwise under the same conditions. It essentially represents the ratio of the levelling off of $R_2/R_2(H=0)$ at full frequency separation of the phonon packets vs. N^* . First, a drop of the ratio of intensities $R_2/R_2(H=0)$ to ~ 0.25 is observed. This is followed by a slight increase, which, in accord with the findings in Ref.1, is caused by spectral diffusion becoming operative at higher bottlenecking. Note, that for spectral diffusion the increase should roughly follow N^{*2} , as observed. To explain the drop to ~ 0.25 in terms of spatial diffusion, we assume that the diffusion constant at full separation is raised by a factor of four relative to zero field due to reduction of resonant Cr^{3+} by a factor of two. Then, from Eqs.(1) and (3),

$$R_2(H=2\text{kG})/R_2(H=0) = \left(\frac{3}{32}\xi^2 + 1\right) / \left(\frac{3}{8}\xi^2 + 1\right), \quad (5)$$

where ξ is the opacity in zero field. According to Fig.2, Eq.(5) is not expected to be valid beyond $\xi \sim 15$. The full drawn curve in Fig.3 is a fit of Eq.(5) to the data with adjustment of the horizontal axis, calibrating N^* in units of the opacity ξ . In particular, it should be noticed that Eq.(5) gives a satisfactory fit, including levelling off at the observed 0.25 without vertical adjustment. For comparison, also the behavior in the ballistic regime, or more precisely the regime of marginal trapping,⁸ is indicated in Fig.3 as the dashed line. Here, by virtue of the reduction of resonant Cr^{3+} by a factor of two in a field, R_2 will go as

$$R_2(H=2\text{kG})/R_2(H=0) = (1 + \frac{1}{2}\xi) / (1 + \xi). \quad (6)$$

The overall conclusion from Fig.3 therefore is, corroborating the findings from Fig.2, that spatial diffusion is predominating from $\xi \sim 2$, somewhat beyond the end of the ballistic regime, up to $\xi \sim 15$, where spectral diffusion sets in.

To summarize, boundary-limited spatial diffusion is found to govern the decay of 29 cm^{-1} phonons at low bottlenecking. The quasi-stationary measuring technique, first described here, appeared to be extremely suitable for obtaining accurate information on weakly bottlenecked optically excited ruby. The technique is, however, not limited to the $2\bar{A}, \bar{E}$ system in ruby, but seems to be quite promising for investigating phonon processes in other optically excited systems as well.

REFERENCES

1. DIJKHUIS J.I., VAN DER POL A, and DE WIJN H.W., *Phys. Rev. Lett.* 37, 1554 (1976).
2. DIJKHUIS J.I. and DE WIJN H.W., to be published.
3. MELTZER R.S. and RIVES J.E., *Phys. Rev. Lett.* 38, 421 (1977).
4. RIVES J.E. and MELTZER R.S., *Phys. Rev. B* 16, 1898 (1977).
5. SUGANO S. and TANABE Y., *J. Phys. Soc. Japan* 13, 899 (1958).
6. MILNE E.A., *J. London Math. Soc.* 1, 40 (1926).
7. KAPLYANSKII A.A., BASUN S.A., RACHIN V.A., and TITOV R.A., *JETP Lett.* 21, 200 (1975).
8. GIORDMAINE J.A. and NASH F.R., *Phys. Rev.* 138, A1510 (1965).